

# Anomalous profile of a self-reversed resonance line from $Ba^+$ in a laser produced plasma from $YBa_2Cu_3O_7$

Riju C. Issac, S.S. Harilal, C.V. Bindhu, Geetha K. Varier, V.P.N. Nampoori, C.P.G. Vallabhan

*Laser Division, International School of Photonics, Cochin University of Science and Technology, Cochin 682 022, India*

Received 4 February 1997; accepted 19 May 1997

## Abstract

A laser produced plasma from the multielement solid target  $YBa_2Cu_3O_7$  is generated using  $1.06\ \mu\text{m}$ , 9 ns pulses from a Q-switched Nd:YAG laser in air at atmospheric pressure. A time resolved analysis of the profile of the  $4554.03\ \text{\AA}$  resonance line emission from Ba II at various laser power densities has been carried out. It has been found that the line has a profile which is strongly self-reversed. It is also observed that at laser power densities equal to or exceeding  $1.6 \times 10^{11}\ \text{W cm}^{-2}$ , a third peak begins to develop at the centre of the self-reversed profile and this has been interpreted as due to the anisotropic resonance scattering (fluorescence). The number densities of singly ionized barium ions evaluated from the width of the resonance line as a function of time delay with respect to the beginning of the laser pulse give typical values of the order of  $10^{19}\ \text{cm}^{-3}$ . The higher ion concentrations existing at smaller time delays are seen to decrease rapidly. The Ba II ions in the ground state resonantly absorb the radiation and this absorption is maximum around 120 ns after the laser pulse. © 1997 Elsevier Science B.V.

**Keywords:** Laser produced plasma; Plasma spectroscopy; Time-resolved spectroscopy; Self-absorption; Self-reversal; Resonance scattering; Resonance fluorescence

## 1. Introduction

The phenomenon of laser ablation, with all its proven potential in material processing, thin film deposition, microelectronics, etc., has evoked considerable interest all over the world in the last couple of decades [1–12]. High quality thin film deposition and better control over film properties have made pulsed laser deposition (PLD) a superior technique in comparison with conventional methods [13–15]. The film thickness, uniformity, stoichiometry, grain size crystallinity, etc. can be controlled with a better precision in PLD [14]. Laser ablation is effectively used for trace analysis in solids by spectral monitoring of laser plasmas [16]. Even though most of the deposition is done in vacuum, Wild and coworkers have reported the deposition of stoichiometric films of

superconducting materials even in the presence of air at atmospheric pressure [17,18]. Due to the high density and collision rate, plasmas formed at high pressure may be considered to be in local thermodynamic equilibrium (LTE) [19]. In this case, emission spectroscopy can effectively and accurately be used for the diagnostics of these plasmas. Apart from these technical applications, laser plasmas can be used as spectral sources for evaluating parameters like oscillator strengths and transition probabilities of atoms and ions [20]. Also these transient fireballs are very useful in studying the basic plasma processes such as the ionization mechanisms, effect of collisions, gas phase reactions etc. [21–24].

Laser plasmas are very rich sources for atomic and ionic emission lines. Line shape analysis can be used in the measurements of plasma parameters in several

ways. Close interactions between an excited atom and an identical ground state atom can cause substantial broadening of the emission lines since the atoms and ions in the ground state absorb the emitted radiation resonantly [19]. Several studies on such resonance scattering of radiation in various types of plasmas have proven to be effective in the determination of the number densities of various emitting species and other parameters like the optical depth and plasma absorption [25–28]. A good knowledge of self-absorption and the optical thickness are necessary for the spectroscopic diagnostics of the plasma [29]. Since the absorption is stronger at the line centre than at the wings, the emission at the central wavelength can be severely absorbed with the interesting result that, in the presence of temperature gradients, the self-reversal of the spectral line will occur [19]. Owing to very high densities of atomic and ionic species in laser produced plasmas, self-absorption effects are severe in such cases, particularly at high enough ambient pressure. There exist a few reports related to self-reversal of spectral lines from laser produced plasmas [7,14,29,30]. The detailed line profile depends critically on the particle density as well as its transport properties in the plasma. The widths of the resonant

lines are as high as a few tens of angstroms and are directly proportional to the density of the emitting species and the absorption oscillator strength [27]. Therefore, the line width is a direct measure of the emitter number density inside the plasma.

Here we report the nature of the emission line profile broadened by self absorption, emission line profile of the resonant transition from Ba II at 4554.03 Å, its evolution in time and its dependence on the laser power density in a laser created plasma from a pellet of superconducting  $\text{YBa}_2\text{Cu}_3\text{O}_7$ . Section 2 describes the basic experimental set-up and in Section 3 the results are discussed and analyzed.

## 2. Experimental details

The schematics of the experimental set-up for the present study are shown in Fig. 1. High power laser radiation from a Q-switched Nd:YAG (Quanta Ray, DCR 11) laser at wavelength 1.06  $\mu\text{m}$ , with a pulse duration of 9 ns, is focused on (focal spot size 50  $\mu\text{m}$  in radius) to the target kept in air at atmospheric pressure to produce the plasma. Laser pulse energy is varied by changing the flash lamp current. The

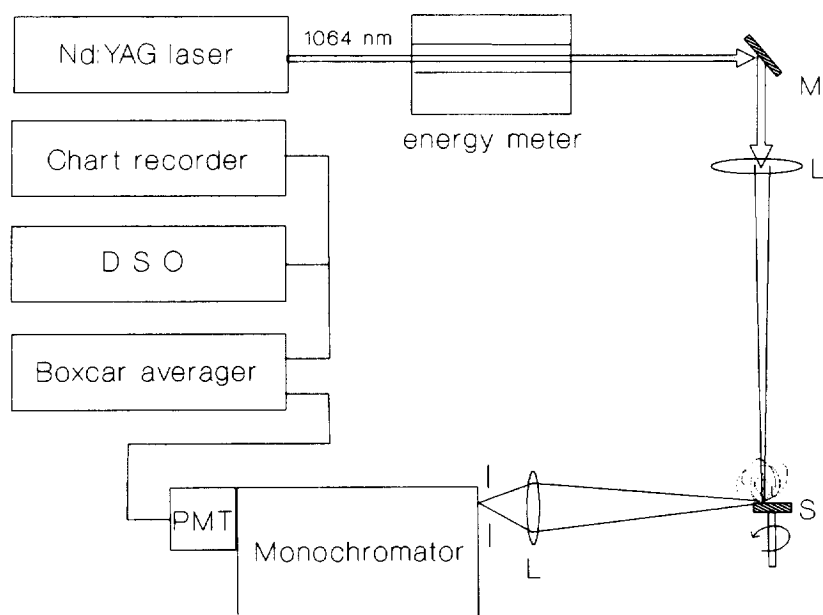


Fig. 1. Schematic representation of the experimental set-up: M, mirror; L, lens; S, sample; PMT, photomultiplier tube; DSO, digital storage oscilloscope.

target used for our studies is a disk of  $\text{YBa}_2\text{Cu}_3\text{O}_7$  of radius 1.75 cm and thickness 0.5 cm which is mounted axially on the shaft of a d.c. motor and it is rotated about the axis in order to avoid multiple hits at the same spot for a long time. The optical emission spectra of the plasma are recorded after one-to-one imaging of the plasma plume on to the entrance slit of a monochromator by appropriate collimating and focusing lenses. Using appropriate slits and apertures, any vertical segment of the plasma situated at definite heights above the target surface can be selected for analysis. The spectrometer used was a 1 m monochromator (SPEX Model:1704, grating with 1200 grooves per mm blazed at 5000 Å, slits 30 μm wide, and slit width limited resolution of 0.15 Å). A thermoelectrically cooled photomultiplier tube (Thorn EMI) was used as the light sensor. Since the transmitted light intensity from the plasma is very high, plume emission occurring at plasma onset and in the first few tens of nanoseconds is enough to saturate the photomultiplier tube. In order to avoid this saturation the photomultiplier is operated at negative high voltage with the anode near ground potential, ie

with 50 Ω characteristic impedance. The spectral recording is done with a chart recorder after averaging intensities from 10 successive pulses using a boxcar averager which can resolve delay times in nanoseconds (Stanford Research Systems, SRS 250). The laser pulse energy is measured with a calibrated laser energy meter and the power density at the focal spot is calculated after making reflection corrections from lens surfaces.

### 3. Results and discussion

A laser ablated plasma from  $\text{YBa}_2\text{Cu}_3\text{O}_7$  in air at atmospheric pressure has been studied and it was found that the spectral emission as well as the ionization mechanism vary with laser power density [24]. Interferometric measurements on the electron density show that it varies in the range  $10^{16}$ – $10^{17}$  cm<sup>-3</sup> depending on the laser power density [24]. The width of the resonance lines are found to be enhanced due to self absorption. Figs 2–4 shows the optical emission spectra in the wavelength range

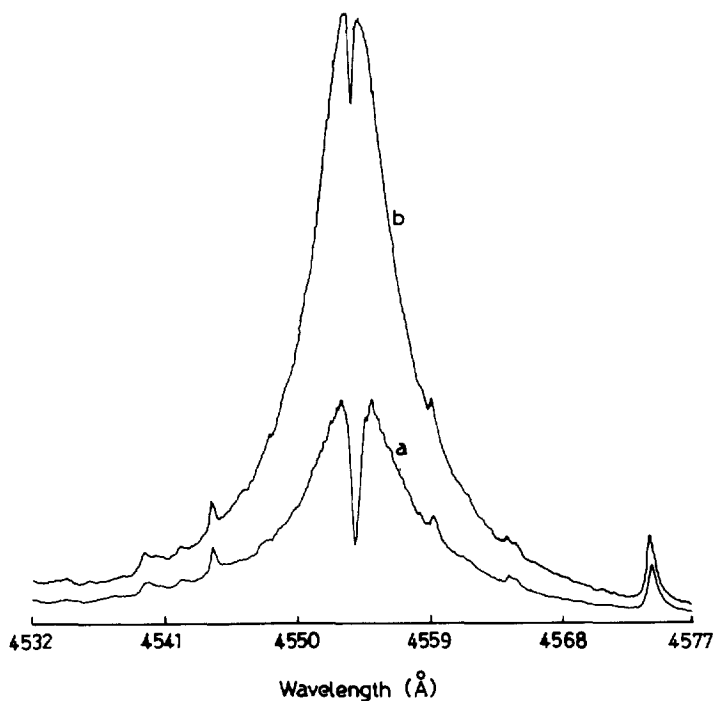


Fig. 2. The resonance broadened and self-reversed profile of the Ba II line of wavelength 4554.03 Å at two laser power densities (a)  $5.4 \times 10^{10}$  W cm<sup>-2</sup> and (b)  $1.2 \times 10^{11}$  W cm<sup>-2</sup>. The radiation intensity at the center of the line increases as the laser power density is increased.

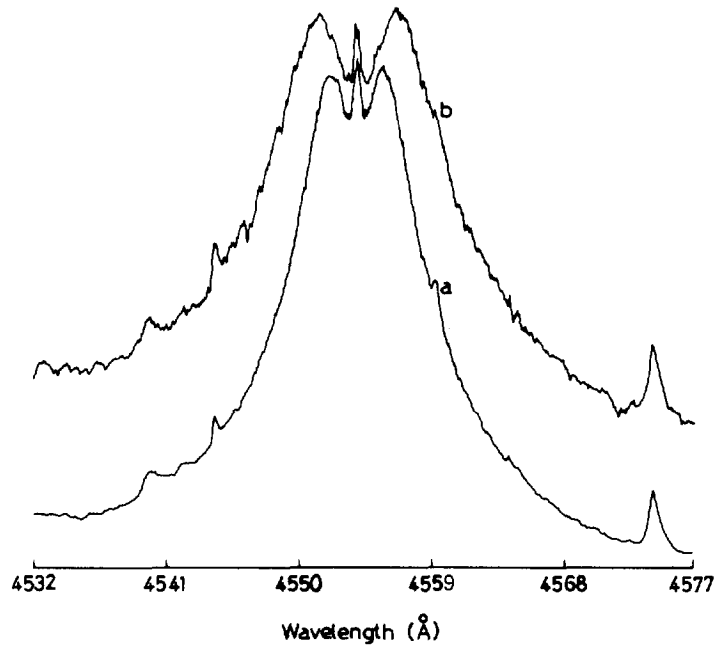


Fig. 3. The profile of the line at 4554.03 Å at laser power densities (a)  $1.6 \times 10^{11} \text{ W cm}^{-2}$  and (b)  $2.4 \times 10^{11} \text{ W cm}^{-2}$ . A third peak at the center of the line is seen at these power densities.

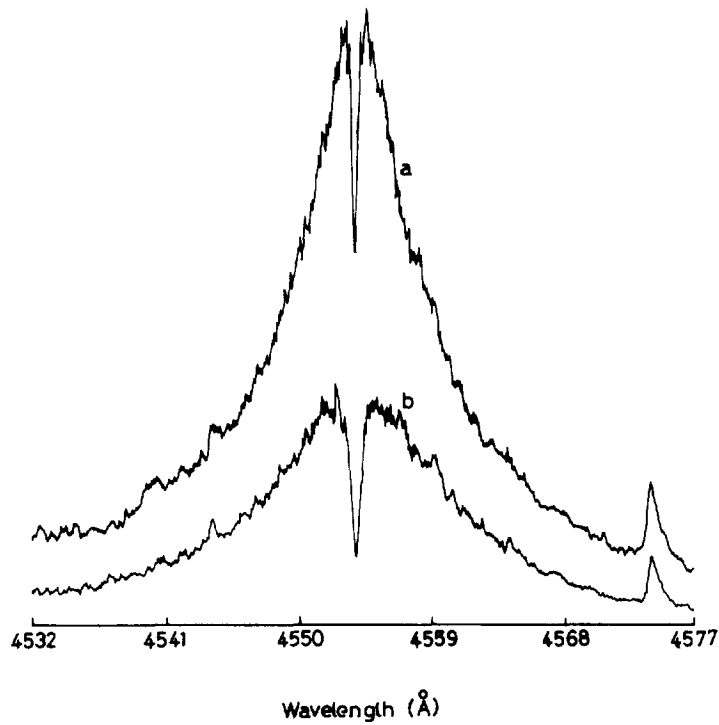


Fig. 4. The 4554.03 Å line profile at laser power densities (a)  $2.6 \times 10^{11} \text{ W cm}^{-2}$  and (b)  $2.7 \times 10^{11} \text{ W cm}^{-2}$ . The profile is similar to that in Fig. 2. Here the plasma as a whole diffuses away from the target surface and the plasma length along the line of sight decreases.

$\lambda = 4532\text{--}4577 \text{ \AA}$  at laser power densities ranging from  $5.4 \times 10^{10} \text{ W cm}^{-2}$  to  $2.7 \times 10^{11} \text{ W cm}^{-2}$  at a distance  $\sim 0.5 \text{ mm}$  from the target. These spectra were recorded with zero time delay after the laser pulse. The spectrum shows the emission profile of the resonant line from singly ionized barium at  $4554.03 \text{ \AA}$  corresponding to the transition  $6p^2P_{3/2} \rightarrow 6s^2S_{1/2}$ . The centre of the line is self-reversed due to the absorption of radiation by the ions in the ground state. Fig. 2 very clearly demonstrates the way in which the line shape develops with the power density. As the laser power density is increased, the intensity at the line centre and the overall width of the spectral line are increased. When the laser power density reached about  $1.6 \times 10^{11} \text{ W cm}^{-2}$ , a third peak begins to develop at the line centre. Fig. 3 shows the line profile at power densities  $1.6 \times 10^{11} \text{ W cm}^{-2}$  and  $2.4 \times 10^{11} \text{ W cm}^{-2}$ . At these power densities the line width increases as the laser power density increases but the line intensity is reduced. That is, the photons from the peak of the line are redistributed into the wings. But when the power density reaches a value  $2.6 \times 10^{11} \text{ W cm}^{-2}$  the plasma as a whole drifts away from the target surface due to the collective diffusion thereby reducing the particle density as well as the plasma length near the target. Then the third peak at the line centre vanishes and a self-reversed profile reappears. Fig. 4 represents such a situation at  $2.6 \times 10^{11} \text{ W cm}^{-2}$  and at  $2.7 \times 10^{11} \text{ W cm}^{-2}$ . This happens because the plasma as a whole collectively drifts away from the target surface thereby reducing the length of the plasma at the observation point. This phenomenon is characterized by a threshold power density and as the power density is increased still further the plasma drifts more and more away from the target and the intensity of emission goes on decreasing as shown in the figure. Under these circumstances the emission intensity maxima is shifted to a distance away from the target surface. Similar effects have been discussed in several other reports and this has been attributed to laser plasma interactions at high laser power densities [31]. In a dense plasma at atmospheric pressure (the one we describe here), the laser plasma interaction depth is limited to the skin depth in the plasma and electrons are heated up by inverse bremsstrahlung. The hot electrons escaping from the plasma can form a charged double layer at the plasma boundary and a part of the

kinetic energy of the electrons is transferred to ions through electrostatic attraction [32,33]. This phenomena is similar to the ambipolar diffusion in plasmas. Ambipolar diffusion is characterised by the collective nature and the diffusion coefficient and hence the velocity of the ions become twice that of the initial value [34]. This phenomena will be discussed in detail elsewhere.

Self-reversal of a spectral line is said to occur when the radiation flux from the system is smaller at the line centre than for the neighbouring wavelengths. The gas temperature inside the core is higher than that near its boundary and there exists a steep gradient in particle density as well as in temperature along the line of sight. For an optically thick plasma with spatially uniform absorption coefficient and assuming a Lorentzian line shape for the spectral line, the radiation flux at an angular frequency  $\omega$  is given by the equation [35],

$$I_{\omega} = I_{\omega}^{(0)} \left( 1 - \frac{e^{-\tau}}{\tau} + \frac{a}{\tau} \right) \quad (1)$$

where  $I_{\omega}^{(0)}$  is the blackbody radiation flux at the line centre given by  $I_{\omega}^{(0)} = (\omega^2/4\pi^2c^2)[\exp(\hbar\omega/kT) - 1]^{-1}$ ,  $\tau$  is the frequency dependent optical depth given by the relation  $\tau = k_0 l \nu^2 / [\nu^2 + (\omega_0 - \omega)^2]$ ,  $T$  (K) is the temperature of the ions,  $k_0$  ( $\text{cm}^{-1}$ ) is the absorption coefficient in the plasma,  $l$  (cm) is the length of the plasma,  $\nu$  (Hz) is the full width at half maximum of the emitted line,  $\omega_0$  (Hz) is the resonance angular frequency, and  $a$  is a temperature dependent quantity given by

$$a = \frac{2}{3} \frac{dT}{dx} l \frac{\hbar\omega}{T^2} (e^{\hbar\omega/T} - 1)^{-1}$$

If  $a \gg e^{-\tau_0}$ ,  $I_{\omega} \gg I_{\omega}^{(0)}$  (optically thick) and if  $a \ll e^{-\tau_0}$ ,  $I_{\omega} \ll I_{\omega}^{(0)}$  (optically thin). That is, when  $a \gg e^{-\tau_0}$ , the radiation flux in the vicinity of the line centre increases while at the centre it is a minimum and the line is self-reversed. The maximum radiation intensity  $I_{\omega_1}$  corresponds to a frequency ( $\omega_1$ ) for which the optical thickness satisfies the condition  $(\tau + 1)e^{-\tau} = a$ . Therefore from Eq. (1),

$$I_{\omega_1} = I_{\omega}^{(0)}(1 + e^{\tau}) \quad (2)$$

From Eq. (2) and using the expression for  $\tau$ , the value of  $k_0 l$  is estimated from the observed line profiles at various time delays after the laser pulse and its value is found to vary between 0.7 and 0.95 as shown in Fig. 5.

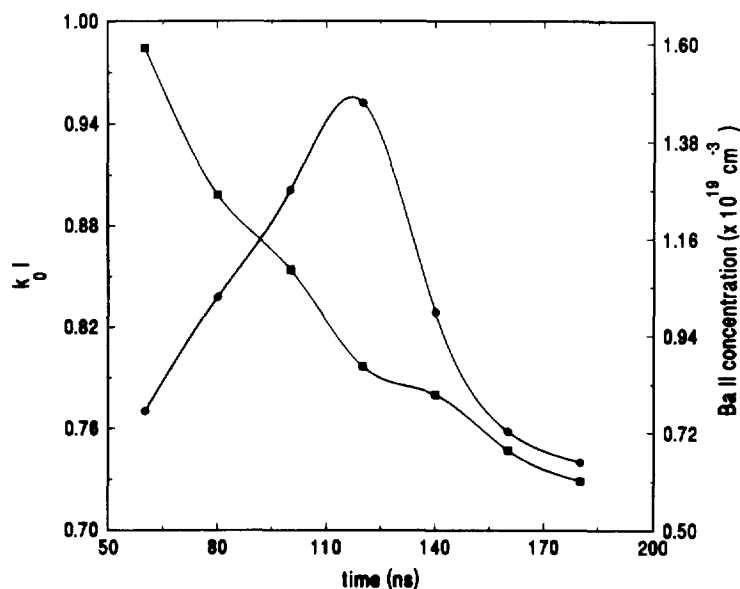


Fig. 5. Variation of the ion number density (■) as well as plasma absorption (●) as a function of time delay after the laser pulse. Number density is maximum at short time delays but plasma absorption peaks about 120 ns after the laser pulse. The data is taken at a laser power density of  $1.2 \times 10^{11} \text{ W cm}^{-2}$ .

The number densities of the species is directly proportional to the full width at half-maximum of the resonant line through the relation [27]

$$\Delta\nu_{\text{res}} = \frac{cr_e}{8} k_{jj'} f_{\text{res}} \lambda_{\text{res}} N \quad (3)$$

where  $r_e$  (cm) is the classical electron radius,  $c$  ( $\text{cm s}^{-1}$ ) is the speed of light in vacuum,  $\lambda_{\text{res}}$  (cm) is the wavelength of the resonant transition,  $f_{\text{res}}$  the resonant oscillator strength,  $N$  ( $\text{cm}^{-3}$ ) the species number density and  $k_{jj'}$ , is a constant determined by the ground and resonance levels. For noble gases with  $j = 0$  and  $j' = 1$ ,  $k_{jj'} = 1.53$  [27]. In order to estimate the plasma absorption and the ion number density, the profile of the line at  $4554.03 \text{ \AA}$  is recorded with a boxcar gate width 10 ns for different time delays after the laser pulse. Using Eq. (3) and taking  $k_{jj'} = 1$ , the number density of Ba II is calculated at various time delays for a typical laser power density of  $6.2 \times 10^{10} \text{ W cm}^{-2}$ . Fig. 5 shows the plot of  $k_0 l$  vs. time delay as well as that between number density and time delay of the barium ions. The ion number density decreases very rapidly at shorter time delays as compared to the decay at later times. However, the value of  $k_0 l$  peaks at around 120 ns after the laser pulse. The low value of

$k_0 l$  at small time delays is expected since during that period the plasma is in a highly dense and ionized state with a large number of collisions with the result that the majority of the ions are in the excited state. The small value of  $k_0 l$  at higher time delays is due to the decrease in the overall ion density in the plasma by electron-ion recombination. This outcome is clear from the low values of the ion number density shown in the figure.

In general, the radiative transfer of energy from the plasma depends on the effective absorption cross-section of the transition, the spontaneous decay rate and the resonance scattering of radiation. Resonance scattering (fluorescence) can occur either with the frequency distribution of the scattered photons the same as that emitted spontaneously (i.e. a Lorentzian function,  $L(\omega, x)$ ) or with a modified distribution characterized by a redistribution function. The frequency redistribution tries to enhance the intensity of the emitted light near the line centre, contrary to the case when the scattered photons have the same frequency distribution as the absorption coefficient [19]. When the spontaneously emitted frequency distribution is not largely modified due to various interactions in the plasma, the ratio of the excitation

rate ( $R_c$ ) to the effective radiative decay rate ( $R_r$ ) is given by [19]

$$\frac{R_r}{R_c} = 2.3 \times 10^{16} \frac{1}{N_e} \left( \frac{\hbar\omega}{E_H} \right)^3 \left( \frac{kT}{E_H} \right)^{1/2} \quad (4)$$

where  $N_e$  ( $\text{cm}^{-3}$ ) is the electron density,  $E_H$  (eV) the ionization potential of hydrogen,  $kT$  (eV) the temperature of ions in the plume and other symbols have the usual meaning. Eq. (4) shows that the ratio  $R_r/R_c$  is inversely proportional to the electron density in the plasma. In the present case, with  $N_e = 10^{16} \text{ cm}^{-3}$  and  $T \sim 13 \text{ eV}$  (corresponding to a velocity of  $3.5 \times 10^5 \text{ cm s}^{-1}$ ),  $(R_r/R_c) = 0.036$ . For small values of  $R_r/R_c$ , the ratio of the population of the upper level to that of the lower level is reduced from its local thermodynamic equilibrium value by a factor  $1 - (R_r/R_c)$  near the line centre frequency [19]. Therefore, the intensity at the line centre is less than that corresponding to frequencies away from the line centre. This explains the self reversal of the lines shown in Figs 2, and 4.

The observation of the central peak in the self-reversed line can be accounted for by the resonant scattering of photons by ions in the ground state with a frequency redistribution. When the scattered photons have a modified frequency distribution (because of anisotropic resonance scattering),

different from that emitted by the ions, the situation is not similar to that described above. The outgoing photons do not have the same frequency distribution as the absorption coefficient and the shape of the line changes considerably. When the resonantly scattered photons have a modified frequency distribution different from that emitted by the ions, the line shape changes considerably. Then the emission intensity has to be averaged over all possible directions and the source function becomes [19]

$$S(\omega, \tau) \approx \frac{\hbar\omega^3 g_n N_m(\tau)}{4\pi^3 c^2 g_m N_n(\tau)} \left( 1 + \frac{1}{6} q \left( 1 - \frac{1}{\pi} \right) + \dots \right) \quad (5)$$

for  $\exp(\hbar\omega/kT) \gg 1$ . Here  $g_m$  and  $g_n$  are the statistical weights of the upper and lower levels and  $q$  the relative probability for resonance scattering. The above equation suggests that scattering tries to enhance the intensity of the resonance line. For frequencies slightly off the line centre, the  $\Theta = -\Theta$  ( $\Theta$  is the scattering angle) direction contributes significantly and the coefficient  $q$  in Eq. (5) is smaller by a factor of  $(\pi - 2)/(\pi - 1) \sim 0.5$ . Therefore the intensity enhancement is prominent at the line centre and this results in the third peak.

Figs 6 and 7 show the time dependence of the line profile of radiation from Ba II at 4554.03 Å. The

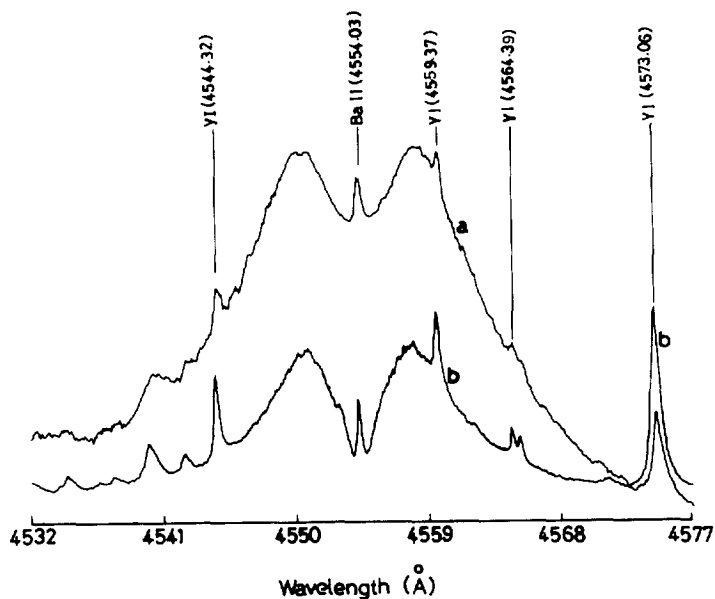


Fig. 6. Line profile at two different time delays after the laser pulse; (a) 30 ns (b) 700 ns at a laser irradiance of  $2.4 \times 10^{11} \text{ W cm}^{-2}$ . The width of the line is substantially reduced at longer time delays, but the central peak become more prominent.

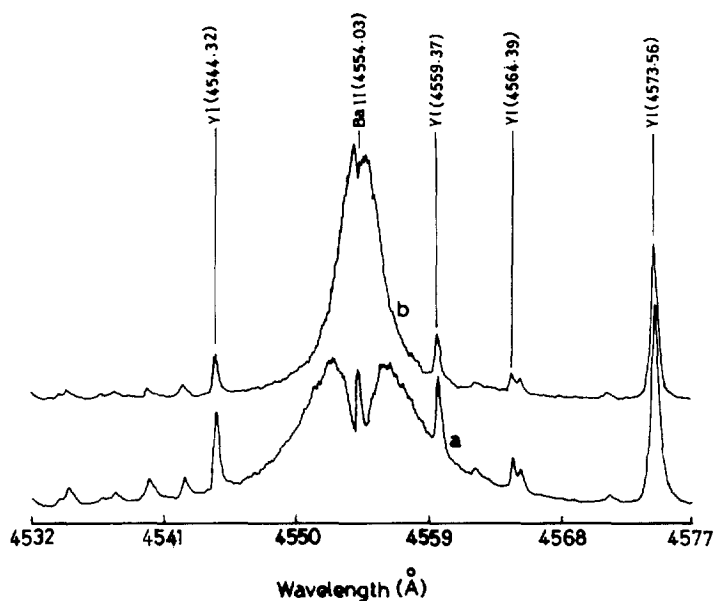


Fig. 7. Line profile at (a) 1.4  $\mu\text{s}$  and (b) 4  $\mu\text{s}$  after the laser pulse. The width of the line is reduced considerably and the peak at the center vanishes.

spectrum was recorded at a laser power density of  $2.4 \times 10^{11} \text{ W cm}^{-2}$  and averaged for about 4  $\mu\text{s}$ . The intensity of the third peak at the line centre increases as the delay time is increased. Also the overall width of the line decreases as time goes on. The full width at half maximum of the third peak is a fraction of an angstrom (namely, 0.26 Å, 700 ns after the laser pulse) and is free from self-absorption broadening. After about 4  $\mu\text{s}$  the width of the entire line is reduced considerably and there is only a very small dip at the line centre since the plasma is becoming optically thin. Some of the emission lines from Y I are also seen which are not so broad and intense and less susceptible to self absorption.

#### 4. Conclusions

The spectral profile of the intense, resonant line emission from Ba II at 4554.03 Å occurring in a laser produced plasma from  $\text{YBa}_2\text{Cu}_3\text{O}_7$  is analyzed. This line is broadened by self-absorption with a full width at half-maximum of several angstroms. The profile becomes self-reversed when sufficient ground state ions exist along the line of sight, because the line has a maximum absorption coefficient at the line

centre. Calculations on the Ba II density and the absorption along the line of sight show that the ion density is maximum during the initial stages of plasma evolution while the resonant absorption peaks after a time delay of about 120 ns. This shows that during the initial stages of plasma evolution, most of the ions are in the excited state. The absorption peaks around 120 ns indicating the abundance of ground state ions at later times. Thereafter the decrease in the particle density inside the plume makes the plasma optically thin and the plasma absorption decreases. As the input laser power density is increased, the resonance scattering in the plasma becomes more anisotropic giving rise to a third peak at the centre of the self-reversed line, whose width is only a fraction of an angstrom.

#### Acknowledgements

The present work is supported by the Department of Science and Technology (Government of India). The authors RCI and CVB are thankful to the University Grants Commission (New Delhi) for their research fellowships and SSH wish to acknowledge the Council of Scientific and Industrial Research (New Delhi) for research fellowship.



## References

- [1] H.F. Smith and A.F. Turner, *Appl. Opt.*, 4 (1965) 147.
- [2] T.N. Lee, W.A. Molander and R.C. Elton, *Phys. Rev. A*, 33 (1986) 1202.
- [3] D.B. Geohegan and D.N. Mashburn, *Appl. Phys. Lett.*, 55 (1989) 345.
- [4] Yasuo Iida, *Spectrochimica Acta B*, 45 (1990) 1353.
- [5] Yueynan Xia, Liangmo Mei, Chunyu Tan, Xiangdong Liu, Qingpu Wang and Shubin Yue, *Appl. Phys. A*, 52 (1991) 425.
- [6] K.H. Wu, C.L. Lee, J.Y. Juang, T.M. Uen and Y.S. Gou, *Appl. Phys. Lett.*, 58 (1991) 1089.
- [7] M. Autin, A. Briand, P. Manchien and J.M. Mermet, *Spectrochimica Acta Part B*, 48 (1993) 851.
- [8] H. Jiang, A.J. Drehman, R.J. Andrews and J.A. Horrigan, *Appl. Phys. Lett.*, 65 (1994) 3132.
- [9] S.S. Harilal, P. Radhakrishnan, V.P.N. Nampoori and C.P.G. Vallabhan, *Appl. Phys. Lett.*, 64 (1994) 3377.
- [10] Ana Ganazalea, Montserrat Ortiz and Jose Campose, *Appl. Spectroscopy*, 49 (1995) 1632.
- [11] L.C. Jensen, S.C. Langford, J.T. Dickinson and R.S. Addeleman, *Spectrochimica Acta B*, 50 (1995) 1501.
- [12] S.S. Harilal, Riju C. Issac, C.V. Bindhu, V.P.N. Nampoori and C.P.G. Vallabhan, *J. Appl. Phys.*, 80 (1996) 3561.
- [13] Rajiv K. Singh and J. Narayan, *Phys. Rev. B*, 41 (1990) 8843.
- [14] D.B. Chrisey and G.K. Hubler (eds.), *Pulsed laser deposition of thin films*, Wiley, New York, 1994.
- [15] J.C. Miller and D.B. Geohegan (eds.), *Laser Ablation: Mechanisms and Applications II*, American Institute of Physics, New York, 1993.
- [16] J.A. Aguilera, C. Aragon and J. Campose, *Appl. Spectroscopy*, 46 (1992) 1382.
- [17] J. Wild, P. Engst, C. Civis, J. Pochyly and J. Pracharova, *Appl. Phys. Lett.*, 60 (1992) 1747.
- [18] J. Wild, P. Bohacek, J. Macl, P. Engst, J. Pracharova and J. Pochyly, *Physica C*, 209 (1993) 486.
- [19] H.R. Griem, *Plasma Spectroscopy*, McGraw Hill, New York, 1964.
- [20] F. Blanco, B. Botho and J. Campose, *Physica Scripta*, 52 (1995) 628.
- [21] W. Pietsch, *J. Appl. Phys.*, 79 (1996) 1250.
- [22] R. Kelly, *Phys. Rev. A*, 46 (1992) 860.
- [23] S.S. Harilal, Riju C. Issac, C.V. Bindhu, Geetha K. Varier, V.P.N. Nampoori and C.P.G. Vallabhan, *Pramana-J. of Phys.*, 46 (1996) 145.
- [24] Geetha K. Varier, Riju C. Issac, S.S. Harilal, C.V. Bindhu, V.P.N. Nampoori and C.P.G. Vallabhan, *Spectrochimica Acta Part B*, 52 (1997) 657.
- [25] J.M. Vaughan, *Phys. Rev. A*, 166 (1968) 13.
- [26] A.R. Malvern, J.L. Nicol and D.N. Stacey, *J. Phys. B*, 7 (1974) L518.
- [27] J. Cedolin, R.K. Hanson and M.A. Capelli, *Phys. Rev. A*, 54 (1996) 335.
- [28] M.R. Winchester and R.K. Marcus, *Spectrochimica Acta Part B*, 51 (1996) 839.
- [29] Y. Leng, J. Goldhar, H.R. Griem and R.W. Lee, *Phys. Rev. E*, 52 (1995) 4328.
- [30] J.F. Kielkopf, *Phys. Rev. E*, 52 (1995) 2013.
- [31] Dieter Baurle, *Laser Processing and Chemistry*, Springer, New York, 1996, p.184.
- [32] S. Eliezer and H. Hora, *Phys. Reports*, 172 (1989) 339.
- [33] E.G. Gamaly, *Laser and Particle Beams*, 12 (1994) 185.
- [34] E.M. Lifshitz and L.P. Pitaevskii, *Physical Kinetics*, Pergamon, Oxford, 1981, p. 108.
- [35] B.M. Smirnov, *Physics of weakly ionized plasmas*, Mir Publishers, Moscow, 1981.